Kottakkal Journal of Ayurvedic Medicine and Research
Volume 2, Issue 3 (July-September) 2026 |Page No: 01-18 | ISSN: 3107-4057

ELUCIDATING THE THERAPEUTIC POTENTIAL OF NATURAL HERB *RUBIA CORDIFOLIA* (*MANJISHTA*) THROUGH *IN SILICO* APPROACH AGAINST THE DRUG TARGETS OF PSORIASIS

[1]Dr.Muhammed.M V, [2]Dr.Benil.P B MD(Ayu), PhD
[1]PG Scholar, [2]Professor and HOD
[1,2]Department of Agadatantra, VPSV Ayurveda College Kottakkal

---

Abstract:

Background: Psoriasis is a chronic immune-mediated inflammatory skin disease with multiple phenotypically distinct subtypes. Therapeutic options for psoriasis include topical therapy, phototherapy or systemic treatment. Treatment targets include at least 75% or 90% improvement in PASI. Despite its growing prevalence, current pharmacological options remain limited. *Manjishta* (*Rubia cordifolia* L), described in classical Ayurvedic literature under *Varnya, Vishaghna* and *Jwarahara mahakashaya*, possesses documented hepatoprotective, anti-inflammatory, anti-proliferative and antioxidant properties. This study aimed to evaluate the potential molecular mechanisms of *Manjishta* phytoconstituents against psoriasis associated targets using in-silico approaches.

Methods: Phytoconstituents of *Rubia cordifolia* L were retrieved from the IMPPAT and PubChem databases. ADME properties and drug-likeness were assessed using SwissADME, and bioavailability was visualized using the Boiled Egg model. Protein–protein interaction (PPI) networks were constructed via STRING. Molecular docking was performed using AutoDock Vina against key psoriasis related proteins. Docking interactions were analyzed in Discovery Studio Visualizer.

Results: Phytoconstituents such as lucidin ethyl ether, xanthopurpurin, 1-hydroxy-2 methoxyanthraquinone, rubiadin, 1-hydroxy-2-methylanthraquinone and 2-(methoxymethyl)-1,3-dihydroxyanthraquinone demonstrated strong binding affinities (−7.0 to −8.4 kcal mol^{-1}) toward estrogen receptor beta, neutrophil elastase, induced myeloid leukemia cell differentiation protein Mcl-1 and M-phase inducer phosphatase. ADME analysis indicated favorable oral bioavailability and compliance with Lipinski's rule of five. The PPI network highlighted ESR1, BCL2, CASP3, DNMT1, TERT, PTPRC, DNMT3A, ESR2, MCL1 and ELANE as central nodes associated with psoriasis pathology, suggesting multi-target modulatory potential.

Conclusion: This in-silico analysis predicts potential interactions of *Rubia cordifolia* phytoconstituents with key apoptotic, anti-inflammatory, anti-proliferative and antioxidant pathways implicated in psoriasis. These findings warrant further experimental research to validate their biological relevance.

Keywords: Bioinformatics, Drug discovery, In-Silico, *Manjishta*, Molecular docking, Network pharmacology, Psoriasis, *Rubia cordifolia*.

Introduction

Rubia cordifolia L, known as *Manjishta* (Figure-1) in Ayurveda, is described in *Caraka Saṃhitā*, under *Varnya, Vishaghna* and *Jwarahara mahākāśaya* and is traditionally indicated in *Visha, Shotha, Akshi ruk, Karna Ruk, Kushta, Visarpa, Vrana* and *Jwara*.[1,2]

Phytochemical investigations have identified alkaloids, tannins, phenols, flavonoids, quinones and terpenes as major class of phyto-constituents. Major bioactive compounds in *Rubia cordifolia*, includes alizarin, munjistin, rubiadin, purpurin, anthraxquinone and xanthopurpurin which are responsible for its widely reported hepatoprotective, antioxidant, anti-inflammatory, and apoptotic activities.[3,4] Psoriasis is a clinically

heterogeneous lifelong skin disease that presents in multiple forms such as plaque, flexural, guttate, pustular or erythrodermic psoriasis.

Figure 1 – *Rubia cordifolia* L (*Manjishta).* a) Habit. b) Dried stem of *Rubia cordifolia* L

In 2014, the World Health Organization recognized psoriasis as a significant non-communicable disease and emphasized the challenges associated with its misdiagnosis, insufficient treatment, and the social stigma experienced by affected individuals. Even psoriasis is an immune-mediated inflammatory disease, it has a major genetic component.[5] The pathogenesis of psoriasis is multifactorial, with genetics being a primary contributor. Environmental triggers such as obesity, stress, beta-blockers, smoking and lithium also have been known to exacerbate psoriasis. Psoriasis manifests in several ways; plaque, flexural, guttate, pustular or erythrodermic psoriasis. The plaque psoriasis is the most common form, which presents as well-demarcated salmon pink plaques with silvery-white scale, typically in a symmetrical distribution and affecting the extensor surfaces (especially elbows and knees), trunk and scalp.[6] Inflammatory cytokines are believed to be the initiators for the onset of psoriasis, hyperproliferation and disturbed keratinocyte differentiation are closely involved in the development and maintenance of the disease process. The epidermal acanthosis and parakeratosis seen in a typical psoriatic lesion are a direct result of hyperproliferation and aberrant differentiation of keratinocytes in the skin. For this very reason, compounds that inhibit keratinocyte proliferation and induce keratinocyte differentiation are effective in the management of psoriasis due to their ability to bring balanced homeostasis to the epidermis. Topical therapy, phototherapy or systemic treatment are the current mainstay treatment practicing in psoriasis.[7] However, current evidence remains largely limited to isolated experimental models focusing on general hepatoprotection rather than psoriasis specific molecular mechanisms. Most available studies explore its anti-inflammatory or antioxidant potential in non-metabolic liver injury, leaving a gap in understanding how phytochemicals of interacts with molecular regulators uniquely implicated in psoriasis such as estrogen receptor beta, Induced myeloid leukemia cell differentiation protein Mcl-1, Neutrophil elastase, Caspase-3, M-phase inducer phosphatase 2, and oxidative stress mediators.[8] Computational approaches such as molecular docking, molecular dynamics (MD) and in-silico ADME prediction provide a powerful tool to elucidate ligand - protein interactions, prioritize pharmacological targets and predict drug-likeness in complex diseases like psoriasis. These tools are particularly valuable in bridging the critical research gap by identifying psoriasis specific molecular targets of phytochemicals, providing mechanistic insights that experimental studies have not yet fully explored. Therefore, integrating classical Ayurvedic knowledge of Manjishta (Rubia cordifolia L) with structure-based in-silico analysis may

help delineate the compound's multi-target apoptotic, anti-hyperproliferative, anti-inflammatory and antioxidant potential and guide rational drug development for psoriasis.

Methods

The bioactive constituents from of *Rubia cordifolia* were first retrieved from the IMPPAT phytochemical database, and their corresponding canonical SMILES structures were obtained from PubChem. These compounds were screened for pharmacokinetic suitability, ADME and drug-likeness using SwissADME (v.3.0), which computes descriptors such as molecular weight, hydrogen-bond donors and acceptors, rotatable bonds, topological polar surface area (TPSA), lipophilicity indices, solubility predictions, gastrointestinal absorption, Blood Brain Barrier permeation, P-gp substrate status, skin permeability coefficient (Log Kp) and bioavailability scores. The "BOILED-Egg" model was used to predict passive intestinal absorption, brain permeation and efflux likelihood. Compounds satisfying Lipinski rule, skin permeability coefficient and P-gp substrate ststus were selected for target identification using Similarity Ensemble Approach (SEA). The target with p value < 0.05 and MaxTC value ≥ 0.6 were selected. In parallel, psoriasis associated genes were mined from GeneCards (v.5.26.0) using the keyword "Psoriasis".[9] The intersection of phytoconstituents predicted targets with psoriasis related genes was identified using Venny (v.2.1).[10] To further evaluate functional associations, overlapping targets were mapped to the STRING database (v.12.5) for Protein - Protein Interaction (PPI) analysis, with networks constructed under *Homo sapiens* restriction and confidence thresholds ≥ 0.4.[11]

The exported Protein - Protein Interaction (PPI) network was visualized in Cytoscape (v.3.10.3), and hub genes were identified using the CytoHubba plugin based on topological parameters such as degree, closeness and betweenness centralities and clustering coefficient.[12,13] Top 10 hub genes were selected for docking as they represent the most biologically influential and highly connected genes in the network, providing a manageable, high-confidence subset that reduces noise, supports standard downstream analyses, aligns with common literature practice and ensures clear visualization. Protein structures corresponding to these hub genes were retrieved from UniProt data base and Protein Data Bank (PDB), selecting high-quality crystallographic models with maximum sequence length and minimum resolution (< 2.0 Å). The protein structures were pre-processed in BIOVIA Discovery Studio 2025 by removing heteroatoms, water molecules, and redundant chains, followed by polar hydrogen addition to optimize geometry and protonation states, consistent with best practices for docking accuracy and saved as PDB format.[14] Then it is further prepared using Auto Dock Tools (ADT) by adding Kollman charges and Computing Gasteiger charge. It was assigned as AD4 type and saved as PDBQT. The Ligand structures were obtained from PubChem Data base and 3 Dimensional Structure Data File (SDF) format was downloaded. Ligands were energy-minimized using the MMFF94 force field (Open Babel GUI v.3.1.1) with steepest descent optimization. Protonation states of both receptor and ligands were assigned corresponding to physiological pH 7.4 using AutoDock Tools (ADT and assigning Gasteiger charges, defining torsional flexibility and saving in PDBQT format. The grid box was selected from the grid and the X, Y and Z coordinates were noted for each protein. Docking was carried out in AutoDock Vina (v1.1.2**)**, with grid boxes defined at the active site (10 Å dimensions, exhaustiveness set to 8), generating nine docking poses per ligand.[15] Binding affinities were reported in kcal mol-1, with thresholds of –6.0 kcal mol-1 or lower considered indicative of strong binding. The resulting docked complexes were split into individual poses and visualized using BIOVIA Discovery Studio 2025, allowing for detailed analysis of binding orientation, hydrogen bonding, hydrophobic contacts, and key amino acid interactions within the receptor active site. These procedures were shown as a flow chart in Figure 2.

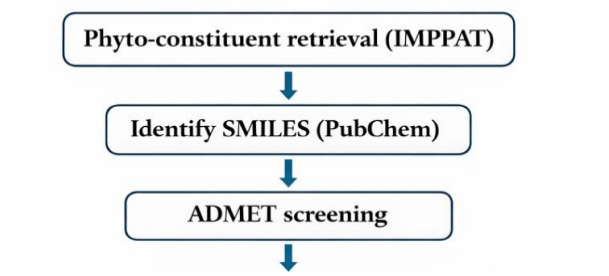

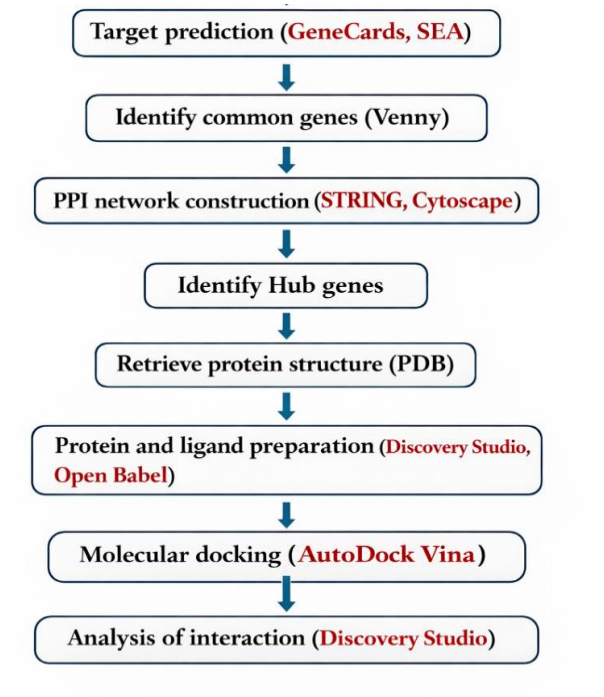

Figure 2 - Flow chart showing the main methodological steps

Results

Total 34 molecules were listed form the IMPPAT database and ADME analysis done through SwissADME provided details of all 34 molecules. The boiled egg diagram of these compounds are given in Figure 3.

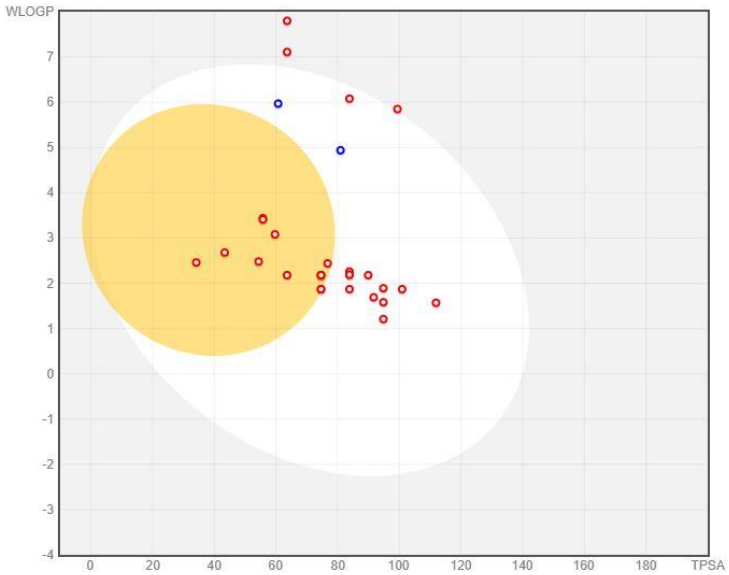

Figure 3 - Boiled egg model

After analyzing the results only 18 molecules were passed the criteria of per Lipinsky rule, Bioavailability score, skin permeability coefficient and Pgp substrate and are given in Table 1.

Table 1 : List of screened molecules with their SMILEs and SwissADME parameter

Sl No	Molecule	SMILE	Formula	MW	H-bond acceptors	H-bond donors	TPSA	GI absorption	BBB permeant	Pgp substrate	Lipinski violations	Bioavailability Score	Log Kp
1.	Dihydromollugin	COC(=O)c1c2CCC(Oc2c2c(c1O)cccc2)(C)C	C17H18O4	286.32	4	1	55.76	High	Yes	No	0	0.55	-5.06
2.	Furomollugin	COC(=O)c1c(O)c2ccccc2c2c1cco2	C14H10O4	242.23	4	1	59.67	High	Yes	No	0	0.55	-5.21
3.	Lucidin ethyl ether	CCOCc1c(O)cc2c(c1O)C(=O)c1c(C2=O)cccc1	C17H14O5	298.29	5	2	83.83	High	No	No	0	0.55	-6.18
4.	1,5-Dihydroxy-2-methylanthracene-9,10-dione	Oc1c(C)ccc2c1C(=O)c1c(C2=O)c(O)ccc1	C15H10O4	254.24	4	2	74.6	High	Yes	No	0	0.55	-4.95
5.	Xanthopurpurin	Oc1cc(O)c2c(c1)C(=O)c1c(C2=O)cccc1	C14H8O4	240.21	4	2	74.6	High	Yes	No	0	0.55	-5.52
6.	Dehydro-alpha-lapachone	O=C1C2=C(C=CC(O2)(C)C)C(=O)c2c1cccc2	C15H12O3	240.25	3	0	43.37	High	Yes	No	0	0.85	-5.93
7.	1-Hydroxy-2-methoxyanthraquinone	COc1ccc2c(c1O)C(=O)c1c(C2=O)cccc1	C15H10O4	254.24	4	1	63.6	High	Yes	No	0	0.55	-5.7
8.	Anthraquinone	O=C1c2ccccc2C(=O)c2c1cccc2	C14H8O2	208.21	2	0	34.14	High	Yes	No	0	0.55	-5.16
9.	1,4-Dihydroxy-2-methylanthraquinone	Oc1c(C)cc(c2c1C(=O)c1ccccc1C2=O)O	C15H10O4	254.24	4	2	74.6	High	Yes	No	0	0.55	-5.28
10.	Alizarin	O=C1c2ccccc2C(=O)c2c1ccc(c2O)O	C14H8O4	240.21	4	2	74.6	High	Yes	No	0	0.55	-5.52
11.	Rubiadin	O=C1c2ccccc2C(=O)c2c1c(O)c(c(c2)O)C	C15H10O4	254.24	4	2	74.6	High	Yes	No	0	0.55	-5.67
12.	Mollugin	COC(=O)c1c2C=CC(Oc2c2c(c1O)cccc2)(C)C	C17H16O4	284.31	4	1	55.76	High	Yes	No	0	0.55	-5.09

13.	Rubilactone	COC(=O)c1c(O)c2ccccc2c2c1ccc(=O)o2	C15H10O5	270.24	5	1	76.74	High	Yes	No	0	0.55	-5.67
14.	1-Hydroxy-2-methylanthraquinone	O=C1c2ccccc2C(=O)c2c1ccc(c2O)C	C15H10O3	238.24	3	1	54.37	High	Yes	No	0	0.55	-5
15.	Physcion	COc1cc(O)c2c(c1)C(=O)c1c(C2=O)c(O)cc(c1)C	C16H12O5	284.26	5	2	83.83	High	No	No	0	0.55	-5.88
16.	2-(Methoxymethyl)-1,3-dihydroxyanthraquinone	COCc1c(O)cc2c(c1O)C(=O)c1c(C2=O)cccc1	C16H12O5	284.26	5	2	83.83	High	No	No	0	0.55	-6.36
17.	1,4-Dihydroxy-5-methoxy-2-methylanthracene-9,10-dione	COc1cccc2c1C(=O)c1c(C2=O)c(O)c(cc1O)C	C16H12O5	284.26	5	2	83.83	High	No	No	0	0.55	-5.48
18.	1,3-Dimethoxy-2-carboxy-anthraquinone	COc1cc2C(=O)c3ccccc3C(=O)c2c(c1C(=O)O)OC	C17H12O6	312.27	6	1	89.9	High	No	No	0	0.56	-6.54

Related genes of these molecules and the psoriasis related genes were tabulated using SEA search server and GeneCards respectively and 18 common genes were identified using Venny 2.0 tools. The Protein-Protein Interaction network for the common genes was constructed using String software (figure 4) and the top 10 genes were plotted using Cytoscape by Maximal Clique Centrality (MCC), Degree Centrality, closeness Centrality and Clustering coefficient (figure 5).

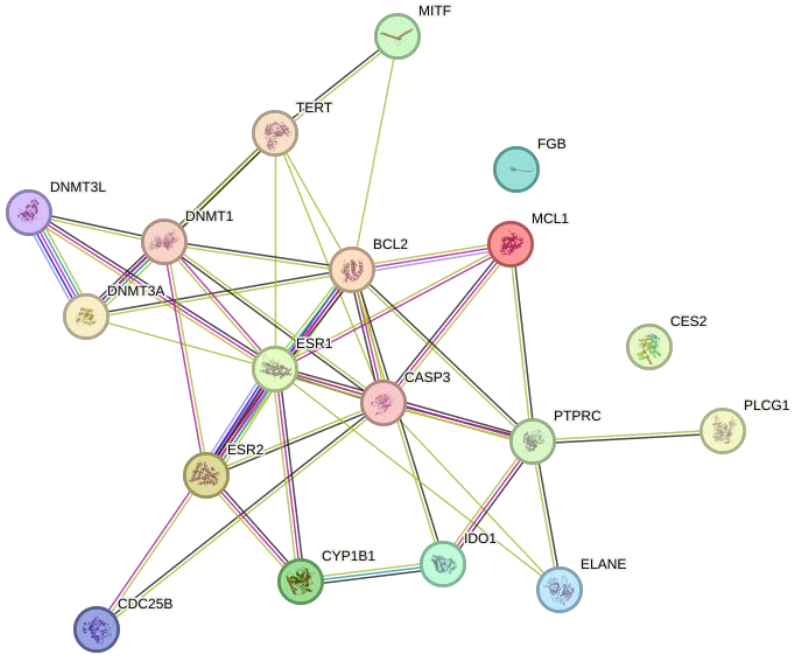

Figure 4 - Protein–Protein Interaction (PPI)

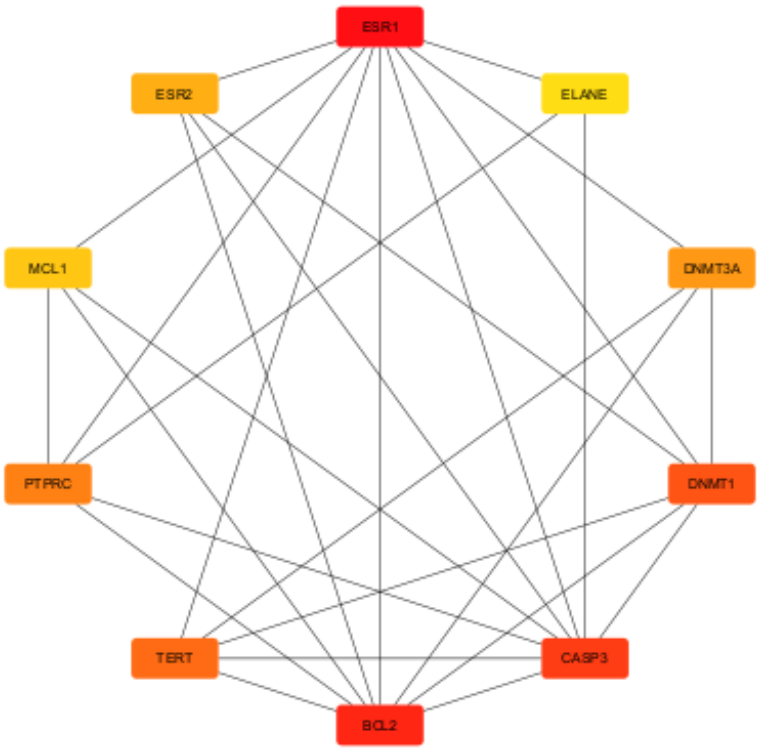

Figure 5 - Hub genes plotted using Cytoscape

Among these, top 10 genes identified through MCC ranking were considered as 10 HUB genes given in table 2, as it measures the involvement of a node within highly interconnected maximal cliques, which reflect biologically meaningful functional modules.

Table 2 – Ranking of top 10 Genes using Cytoscape based on Maximal Clique Centrality, Degree distribution and Clustering coefficient

Rank	MCC	Closeness centrality	Clustering coefficient	Betweenness centrality
1	ESR1	ESR1	ELANE	ESR1
2	BCL2	BCL2	DNMT3L	BCL2
3	CASP3	CASP3	MITF	PTPRC
4	DNMT1	PTPRC	CDC25B	CASP3
5	TERT	DNMT1	MCL1	TERT
6	PTPRC	TERT	DNMT3A	DNMT1
7	DNMT3A	ESR2	ESR2	IDO1
8	ESR2	DNMT3A	TERT	ESR2
9	MCL1	MCL1	DNMT1	CYP1B1
10	ELANE	ELANE	CASP3	DNMT3A

The related phytochemicals were identified for each gene and their canonical smiles, PubChem ID, chemical structure, gene symbol and gene name, and RCSB PDB ID are given in table 3. Total 9 among 18 phytochemicals showed interactions with six target genes; MCL1, ESR2, ELANE, CDC25B, CASP3 and MITF, which are the major genes involved in pathways related to psoriasis.

Table 3: Details of 10 HUB genes their related proteins and phytochemicals

Sl No	Phytochemical	Canonical SMILES	PubChem ID (Compound CID)	Chemical structure	Gene Symbol	Gene Name	RCSB PDB ID
1	Lucidin ethyl ether	CCOCc1c(O)cc2c(c1O)C(=O)c1c(C2=O)cccc1	28578	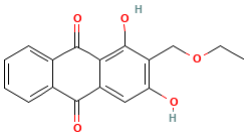	MCL1	Induced myeloid leukemia cell differentiation protein Mcl-1	4HW3
2	Xanthopurpurin	Oc1cc(O)c2c(c1)C(=O)c1c(C2=O)cccc1	196978	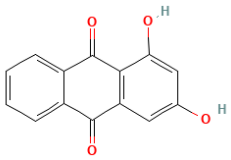	MCL1	Induced myeloid leukemia cell differentiation protein Mcl-1	4HW3
3					ESR2	Estrogen receptor beta	5TOA
4	1-Hydroxy-2-methoxyanthraquinone	COc1ccc2c(c1O)C(=O)c1c(C2=O)cccc1	80103	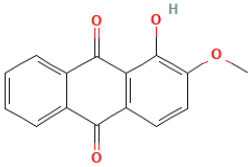	ELANE	Neutrophil elastase	5A8Y
5					MCL1	Induced myeloid leukemia cell differentiation protein Mcl-1	4HW3
6	Anthraquinone	O=C1c2ccccc2C(=O)c2c1cccc2	6780	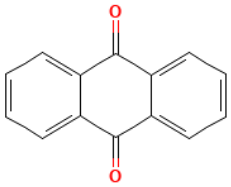	CDC25B	M-phase inducer phosphatase 2	4WH7
7					CASP3	Caspase-3	3DEI
8					MCL1	Induced myeloid	4HW3

						leukemia cell differentiation protein Mcl-1	
9	Alizarin	O=C1c2ccccc2C(=O)c2c1ccc(c2O)O	6293	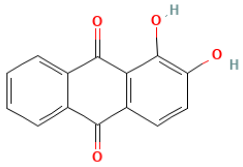	MCL1	Induced myeloid leukemia cell differentiation protein Mcl-1	4HW3
10					MITF	Microphthalmia-associated transcription factor	9H5F
11	Rubiadin	O=C1c2ccccc2C(=O)c2c1c(O)c(c(c2)O)C	124062	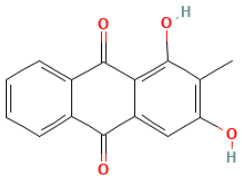	MCL1	Induced myeloid leukemia cell differentiation protein Mcl-1	4HW3
12	1-Hydroxy-2-methylanthraquinone	O=C1c2ccccc2C(=O)c2c1ccc(c2O)C	160817	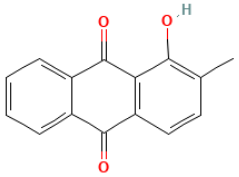	MCL1	Induced myeloid leukemia cell differentiation protein Mcl-1	4HW3
13					MITF	Microphthalmia-associated transcription factor	9H5F

14	Physcion	COc1cc(O)c2c(c1)C(=O)c1c(C2=O)c(O)cc(c1)C	10639	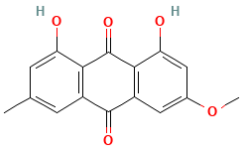	ELANE	Neutrophil elastase	5A8Y
15	2-(Methoxymethyl)-1,3-dihydroxyanthraquinone	COCc1c(O)cc2c(c1O)C(=O)c1c(C2=O)cccc1	149782	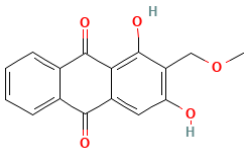	MCL1	Induced myeloid leukemia cell differentiation protein Mcl-1	4HW3

The genes that regulate apoptosis and keratinocyte survival, MCL1 and CASP3; genes such as ELANE which regulate immune-mediated inflammatory responses; genes like ESR2 which regulates hormonal signaling especially cytokine signaling and skin homeostasis form the major cluster, with their proteins. These genes were showed overlap with protein targets like lucidin ethyl ether, xanthopurpurin, 1-hydroxy-2-methoxyanthraquinone, anthraquinone, alizarin, rubiadin, 1-hydroxy-2-methylanthraquinone, physcion and 2-(methoxymethyl)-1,3-dihydroxyanthraquinone. Among these genes, MCL1 demonstrated affinity for majority of compounds; lucidin ethyl ether, xanthopurpurin, 1-hydroxy-2-methoxyanthraquinone, alizarin, rubiadin, 1-hydroxy-2-methylanthraquinone and anthraquinone. ELANE showed affinity with 1-hydroxy-2-methoxyanthraquinone and physcion, where MITF demonstrated affinity with alizarin and 1-hydroxy-2-methylanthraquinone. ESR2 showed affinity with Xanthopurpurin, CDC25B and CASP3 demonstrated connection with anthraquinone. The docking results given in table 4 indicate that several constituents of *Rubia cordifolia* display predicted binding with variety of genes involved in apoptosis regulation, immune and inflammatory regulation, and hormonal and signaling regulation implicated in psoriasis. Notably, xanthopurpurin showed relatively strong predicted binding to ESR2 (−8.4 kcal mol^{-1}) and anthraquinone with MCL1 (−8.3 kcal mol^{-1}). MCL1 also showed high affinity with 1-hydroxy-2-methylanthraquinone (-7.6 3 kcal mol^{-1}); xanthopurpurin (-7.5 kcal mol^{-1}); lucidin ethyl ether, alizarin and rubiadin (-7.4 kcal mol^{-1}); 1-hydroxy-2-methoxyanthraquinone (-7.3 kcal mol^{-1}) and a binding affinity of -7.1 kcal mol^{-1} with 2-(methoxymethyl)-1,3-dihydroxyanthraquinone. ELANE exhibited meaningful affinities against 1-hydroxy-2-methoxyanthraquinone (-6.8 kcal mol^{-1}) and physcion (-6.1 kcal mol^{-1}). The compound anthraquinone showed a good affinity with CASP3 and CDC25B with a binding affinity -6.9 kcal $mol^{-1}$and -6.8 kcal mol-1 respectively. The gene MITF shows the least affinity with alizarin (-4.1 kcal mol^{-1}) and 1-hydroxy-2-methylanthraquinone (-4.2 kcal mol^{-1}).

Table 4: Table showing the Binding affinity of selected ligands with respective targets and their interactions

Sl No	Protein	Ligand	Binding affinity (kcal mol^{-1})	Number of bonds	Name of bond	Category	Type of bonds	Bond distance(Å)	2D molecular interaction diagram
1	MCL1	Lucidin ethyl ether	-7.4	5	A:ARG263 A:VAL253 A:VAL253 A:THR266 A:THR266	Hydrogen bond Hydrophobic Hydrophobic Hydrophobic Hydrophobic	Conventional Pi sigma Pi sigma Pi sigma Pi sigma	3.03763 3.28926 3.62874 3.81226 3.44853	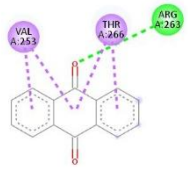
2	MCL1	Xanthopurpurin	-7.5	5	A:VAL253 A:THR266 A:MET231 A:VAL253 A:VAL253	Hydrophobic Hydrophobic Other Hydrophobic Hydrophobic	Pi sigma Pi sigma Pi-Sulfur Pi-Alkyl Pi-Alkyl	3.31481 3.46766 5.61315 5.41824 4.21766	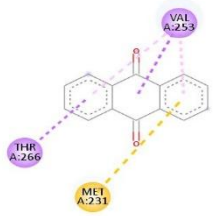
3	MCL1	1-Hydroxy-2-methoxyanthraquinone	-7.3	4	A:VAL253 A:VAL253 A:THR266 A:LEU267	Hydrophobic Hydrophobic Hydrophobic Hydrophobic	Pi-Sigma Pi-Sigma Pi-Sigma Pi-Alkyl	3.44678 3.9721 3.46894 5.40111	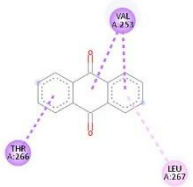
4	MCL1	Anthraquinone	-8.3	11	A:PHE270 A:PHE270 A:VAL249 A:MET231 A:MET250 A:VAL253	Hydrophobic Hydrophobic Hydrophobic Hydrophobic Hydrophobic Hydrophobic	Pi-Pi T shaped Pi-Pi T shaped Amide-Pi Stacked Pi-Alkyl Pi-Alkyl Pi-Alkyl Pi-Alkyl Pi-Alkyl Pi-Alkyl	5.03144 4.61641 4.2872 5.21758 5.17823 4.79365	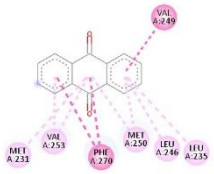

					A:VAL253 A:LEU235 A:LEU246 A:VAL249 A:MET250	Hydrophobic Hydrophobic Hydrophobic Hydrophobic Hydrophobic	Pi-Alkyl Pi-Alkyl	4.90011 5.22983 5.1179 5.03589 4.37603	
5	MCL1	Alizarin	-7.4	6	A:VAL253 A:VAL253 A:THR266 A:THR266 A:ALA227 A:LEU267	Hydrophobic Hydrophobic Hydrophobic Hydrophobic Hydrophobic Hydrophobic	Pi-Sigma Pi-Sigma Pi-Sigma Pi-Sigma Pi-Alkyl Pi-Alkyl	3.86964 3.80245 3.97988 3.75396 4.85438 5.23146	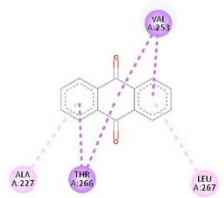
6	MCL1	Rubiadin	-7.4	6	A:VAL253 A:VAL253 A:THR266 A:MET231 A:HIS224 A:VAL253	Hydrophobic Hydrophobic Hydrophobic Other Hydrophobic Hydrophobic	Pi-Sigma Pi-Sigma Pi-Sigma Pi-Sulfur Pi-Alkyl Pi-Alkyl	3.92663 3.30568 3.56492 5.43088 4.81969 4.30166	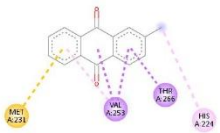
7	MCL1	1-Hydroxy-2-methylanthraquinone	-7.6	8	A:ARG263 A:VAL253 A:VAL253 A:THR266 A:MET250 A:LEU267 A:PHE270 A:LEU267	Hydrogen Bond Hydrophobic Hydrophobic Hydrophobic Hydrophobic Hydrophobic Hydrophobic Hydrophobic	Conventional Pi-Sigma Pi-Sigma Pi-Sigma Alkyl Alkyl Pi-Alkyl Pi-Alkyl	2.25576 3.63152 3.85844 3.67667 5.02269 4.64081 5.30662 5.39288	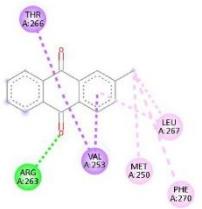

8	MCL1	2-(Methoxymethyl)-1,3-dihydroxyanthraquinone	-7.1	5	A:ARG263 A:VAL253 A:VAL253 A:THR266 A:THR266	Hydrogen Bond Hydrophobic Hydrophobic Hydrophobic Hydrophobic	Conventional Pi-Sigma Pi-Sigma Pi-Sigma Pi-Sigma	3.05571 3.29315 3.61006 3.83089 3.44132	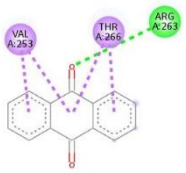
9	ELANE	1-Hydroxy-2-methoxyanthraquinone	-6.8	5	A:CYS220 A:PHE192 A:PHE192 A:VAL216 A:VAL216	Other Hydrophobic Hydrophobic Hydrophobic Hydrophobic	Pi-Sulfur Pi-Pi Stacked Pi-Pi Stacked Pi-Alkyl Pi-Alkyl	5.89955.25739 4.34309 5.07109 4.16925	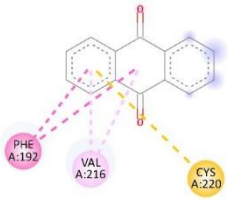
10	ELANE	Physcion	-6.1	7	A:VAL216 A:HIS57 A:PHE192 A:HIS57 A:VAL216 A:PHE192 A:VAL216	Hydrogen Bond Hydrogen Bond Hydrophobic Hydrophobic Hydrophobic Hydrophobic Hydrophobic	Conventional Carbon Hydrogen Bond Pi-Pi Stacked Pi-Pi T-shaped Alkyl Pi-Alkyl Pi-Alkyl	2.32893 3.37839 4.55579 5.29183 3.79962 4.1943 5.31399	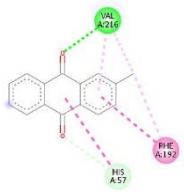
11	MITF	Alizarin	-4.1	3	B:ARG284 B:ARG284 C:LEU282	Hydrogen Bond Hydrogen Bond Hydrophobic	Conventional Carbon Hydrogen Bond Pi-Alkyl	2.07449 3.41145 4.49314	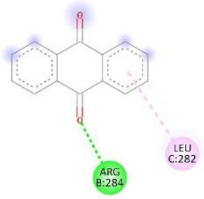
12	MITF	1-Hydroxy-2-methylanthraquinone	-4.2	4	B:ARG284 B:ARG284 B:HIS280	Hydrogen Bond Hydrogen Bond	Conventional Carbon Hydrogen Bond Pi-Alkyl Pi-Alkyl	2.11165 3.46387 4.7228	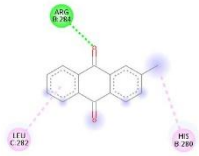

					C:LEU282	Hydrophobic Hydrophobic		4.49711	
13	ESR2	Xanthopurpurin	-8.4	6	B:PHE356 B:PHE356 B:LEU298 B:ALA302 B:LEU339 B:LEU298	Hydrophobic Hydrophobic Hydrophobic Hydrophobic Hydrophobic Hydrophobic	Pi-Pi T-shaped Pi-Pi T-shaped Pi-Alkyl Pi-Alkyl Pi-Alkyl Pi-Alkyl	5.45469 5.10697 5.07621 4.83224 4.50972 5.11088	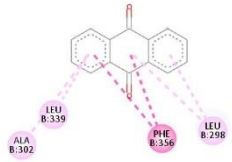
14	CDC25B	Anthraquinone	-6.8	11	A:CYS484 A:ARG485 A:ARG488 A:ARG488 A:ASP397 A:LEU398 A:ARG488 A:ARG488 A:MET505 A:ARG485 A:ARG488	Hydrogen Bond Hydrogen Bond Electrostatic Electrostatic Electrostatic Hydrophobic Hydrophobic Hydrophobic Hydrophobic Hydrophobic Hydrophobic	Conventional Electrostatic Pi-Cation Pi-Cation Pi-Cation Pi-Anion Pi-Alkyl Pi-Alkyl Pi-Alkyl Pi-Alkyl Pi-Alkyl	2.25356 3.84527 3.46584 3.87412 4.35441 5.13364 5.46051 4.33423 5.43026 4.78735 4.48221	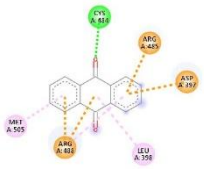
15	CASP3	Anthraquinone	-6.9	4	A:GLY122 A:OCS163 A:SER205 A:HIS121 A:OCS163	Hydrogen Bond Hydrogen Bond Hydrogen Bond Hydrogen Bond	Conventional Conventional Carbon Hydrogen Bond Carbon Hydrogen Bond	2.76645 2.5366 3.73729 3.42865	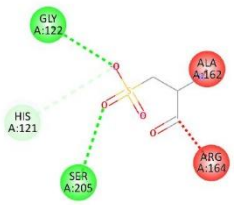

					A:SER205 A:OCS163				

Discussion

Inflammatory cytokines are believed to be the initiators for the onset of psoriasis, and hyperproliferation and disturbed keratinocyte differentiation are closely involved in the development and maintenance of the disease process.[7] The epidermal acanthosis and parakeratosis seen in a typical psoriatic lesion are a direct result of hyperproliferation and aberrant differentiation of keratinocytes in the skin. For this very reason, compounds that inhibit keratinocyte proliferation and induce keratinocyte differentiation and apoptosis are effective in the management of psoriasis due to their ability to bring balanced homeostasis to the epidermis. Today, discovery of more effective and safer anti-proliferative and keratinocyte differentiation-modulating agents remains a worthy scientific pursuit in psoriasis research. *Rubia cordifolia,* a commonly indicated drug in dermatological conditions in Ayurveda, as this drug mentioned in classics under *Varnya, Vishaghna* and *Jwara Hara Maha Kashaya* in *Charaka Samhitha*.[2] It is also indicated in various other conditions such as *Kushta, Visarpa, Shotha* and *Vrana* where hyper proliferation of cells and inflammatory dysregulations are prominent.[1] To establish the role of *Rubia cordifolia* in multiple disease pathologies, computational methods like molecular docking and network analysis are more useful than conventional time consuming experimental methods. In the present study, docking analysis indicated that selected phytochemicals of *Rubia cordifolia* interact with several genes such as MCL1, ESR2, ELANE, CDC25B, CASP3, and MITF associated with pathways involving immune regulation, apoptosis, inflammation, and keratinocyte proliferation relevant to psoriasis**.** The phytochemical, xanthopurpurin showed relatively strong predicted binding to ESR2 (Estrogen receptor beta) with a binding affinity of −8.4 kcal mol^{-1}, which regulates skin inflammation and immune response. MCL1 (Induced myeloid leukemia cell differentiation protein Mcl-1), is an anti-apoptotic BCL2 family protein, which resist programmed cell death by maintaining mitochondrial membrane integrity. In psoriasis, increased MCL1 expression may prolong the survival of keratinocytes, which contributes to the accumulation of epidermal cells in psoriatic plaques. Overexpression of MCL1 may therefore enhance epidermal hyperplasia and also influence immune cell survival within inflamed skin tissue. Through these mechanisms, MCL1 contributes to sustained inflammation and abnormal skin thickening in psoriasis.[16] Molecular docking demonstrated that, the phytochemical, anthraquinone strongly bound with MCL1with a notable binding energy -8.3 kcal mol^{-1}, implies that anthraquinone might be inducing apoptosis results in reduction in epidermal thickness in psoriasis. It also binds with Lucidin ethyl ether, xanthopurpurin, 1-Hydroxy-2-methoxyanthraquinone, alizarin, rubiadin, 1-hydroxy-2-methylanthraquinone and 2-(methoxymethyl)-1,3-dihydroxyanthraquinone with high binding energy less than -6 kcal mol^{-1}, suggestive of probable inhibition of abnormal epidermal hyperplasia observed in psoriasis. The gene ELANE which encodes neutrophil elastase, released by activated neutrophils which are prominent immune cells found in psoriatic lesions. Increased neutrophil elastase activity can intensify inflammatory responses in the skin. ELANE plays an important role in the formation of these neutrophil aggregates within the epidermis and form Munro micro abscesses. This enzyme may also activate inflammatory cytokines and signaling molecules by which ELANE amplifies inflammation and tissue damage in psoriatic skin.[17,18] Phytochemicals 1-hydroxy-2-methoxyanthraquinone and physcion binds to this gene with an affinity of -6.8 kcal mol^{-1} and -6.1 kcal mol^{-1} respectively, explains the probable anti -inflammatory action of *Rubia cordifolia* in psoriasis. ESR2 encodes estrogen receptor beta, a nuclear hormone receptor involved in gene regulation. It plays a role in modulating inflammatory and immune responses in skin tissues. Estrogen signaling through ESR2 can influence cytokine production and immune cell activity. An Altered ESR2 signaling has been suggested to affect the balance of pro-inflammatory mediators, thereby potentially contributing to the chronic inflammatory state of psoriasis, which could partly explain variations in psoriasis severity. It may also affect oxidative stress responses in skin cells which contribute to immune imbalance in psoriasis.[19] Xanthopurpurin, a major phytochemical in *Rubia cordifolia* bound with ESR2 with a binding energy of -8.4 kcal mol^{-1} indicating its predictive anti-inflammatory, antioxidant activity and inhibition of keratinocyte proliferation, a key pathological event involved in psoriasis. CASP3 encodes caspase-3, a key executioner enzyme in the apoptosis pathway,

regulates programmed cell death, and participate in inflammatory signalling cascades. Its altered activity may disturb the balance between keratinocyte proliferation and apoptosis in psoriasis. Balanced apoptosis is necessary for maintaining normal epidermal homeostasis. In psoriasis, keratinocytes often show resistance to apoptosis. Altered CASP3 activity disrupt the normal removal of damaged or excess cells contributes to excessive epidermal cell accumulation.[20] Anthraquinone present in the *Rubia cordifolia* strongly bound with CASP3 with a binding energy of -6.9 kcal mol^{-1} suggestive of its probable role to induce apoptosis which may prevent excessive epidermal cell accumulation. CDC25B is a cell cycle regulatory phosphatase that controls the transition of cells from the G2 phase to mitosis, and its dysregulation may enhance keratinocyte proliferation, a hallmark feature of psoriasis. Overexpression or dysregulation of CDC25B can accelerate epidermal cell cycle progression, thereby contributing to the rapid turnover leading to the formation of thick scaly plaques in psoriasis.[21,22] Molecular docking showed that, Anthraquinone binds with CDC25B gene with a binding affinity of -6.8 kcal mol^{-1}, which refers that anthraquinone inhibits CDC25B may potentially reduce abnormal cell proliferation**,** which is relevant in psoriasis. MITF (Microphthalmia-associated transcription factor) is involved in melanocyte differentiation and immune regulation, and its altered expression may influence inflammatory signaling and pigmentation changes observed in some psoriatic lesions.[23] The phytochemicals alizarin and 1-hydroxy-2-methylanthraquinone bound with MITF with a binding affinity of -4.1 kcal mol^{-1} and -4.2 kcal mol^{-1} showing a weak interaction implies less influence of these compounds in melanocyte differentiation and immune regulation in psoriasis. On an overall analysis of the molecular docking of phytochemicals from *Rubia cordifolia*, it shows its activity on multiple drug targets related to psoriasis, both established and weakly established ones.

Docking generates hypotheses about probable binding modes and relative affinities under simplified conditions; it does not prove biological efficacy. Specific limitations in our study include use of static protein conformations (single PDB snapshots), neglect of full solvation and entropic effects, and no explicit inclusion of protein flexibility or induced fit. These factors can change binding free energy substantially. In addition, in vitro and in vivo effective concentrations depend on ADME (absorption, distribution, metabolism, and excretion), protein expression levels, bio availability of the phytoconstituents in plant extracts, and metabolite formation, none of which are captured by docking alone.

The study recommends a structured validation pathway to support the predictive docking results. First, the actual levels and bioavailable forms of lucidin ethyl ether, xanthopurpurin, 1-Hydroxy-2-methoxyanthraquinone, anthraquinone, alizarin, rubiadin, 1-hydroxy-2-methylanthraquinone, physcion and 2-(methoxymethyl)-1,3-dihydroxyanthraquinone in *Rubia cordifolia* extracts should be quantified using LC-MS/MS. Molecular dynamics simulations (100–200 ns) should then be conducted to evaluate the stability and solvation behaviour of key ligand–protein complexes. Advanced computational techniques like KEGG pathway analysis and gene ontology analysis can also be performed for predicting the possible action of these molecules in each pathway. Finally, anti-inflammatory and antioxidant effects must be tested in relevant cellular models, with in vivo studies undertaken only after confirming in vitro safety and bioavailability.

Conclusion

The docking analysis predicts that key phytochemicals of *Rubia cordifolia* that interact with genes related to apoptosis and keratinocyte survival, immune-mediated inflammatory responses, and hormonal signaling especially cytokine signaling and skin homeostasis in psoriasis, offering a plausible molecular basis for its classical Ayurvedic actions in antitoxic effect, inflammation modulation and maintaining skin homeostasis. These findings are preliminary and hypothesis generating, and docking alone cannot confirm biological efficacy. Experimental validation including phytochemical quantification, functional enzyme and transporter assays, molecular dynamics, and cellular models are essential for next level evidence generation of therapeutic relevance or clinical applicability.

References

1. Mishra BP. Bhavprakash Nighantu Edited by Padmashree Pro. Krushnachandra Chunekar. Reprint Edition. Chaukhambha Bharati Academy. 2022.
2. Charak Samhita Sutrasthana, Shadavirechanashatasriteeya Adhyaya, 4/8,16,39. Available from: http://niimh.nic.in/ebooks/echarak. [Last accessed on 2026 Mar 09].

3. Wen M, Chen Q, Chen W, Yang J, Zhou X, Zhang C, Wu A, Lai J, Chen J, Mei Q, Yang S. A comprehensive review of Rubia cordifolia L.: Traditional uses, phytochemistry, pharmacological activities, and clinical applications. Frontiers in pharmacology. 2022 Sep 9;13:965390.
4. Humbare RB, Sarkar J, Kulkarni AA, Juwale MG, Deshmukh SH, Amalnerkar D, Chaskar M, Albertini MC, Rocchi MB, Kamble SC, Ramakrishna S. Phytochemical characterization, antioxidant and anti-proliferative properties of Rubia cordifolia L. extracts prepared with improved extraction conditions. Antioxidants. 2022 May 20;11(5):1006.
5. Raharja A, Mahil SK, Barker JN. Psoriasis: a brief overview. Clinical Medicine. 2021 May 1;21(3):170-3.
6. Armstrong AW, Read C. Pathophysiology, clinical presentation, and treatment of psoriasis: a review. Jama. 2020 May 19;323(19):1945-60.
7. Armstrong AW, Read C. Pathophysiology, clinical presentation, and treatment of psoriasis: a review. Jama. 2020 May 19;323(19):1945-60.
8. Lin ZX, Jiao BW, Che CT, Zuo Z, Mok CF, Zhao M, Ho WK, Tse WP, Lam KY, Fan RQ, Yang ZJ. Ethyl acetate fraction of the root of Rubia cordifolia L. inhibits keratinocyte proliferation in vitro and promotes keratinocyte differentiation in vivo: potential application for psoriasis treatment. Phytotherapy research. 2010 Jul;24(7):1056-64.
9. ref-Marilyn Safran, Naomi Rosen, Michal Twik, Ruth BarShir, Tsippi Iny Stein, Dvir Dahary, Simon Fishilevich, Doron Lancet. GeneCards Version 5: The comprehensive knowledgebase for human genes. Database. 2021;2021:baab111.
10. Oliveros JC. Venny: An interactive tool for comparing lists with Venn diagrams. BioinfoGP, CNB-CSIC. 2007–2015. Available at: http://bioinfogp.cnb.csic.es/tools/venny/.
11. Huerta-Cepas J, Simonovic M, Doncheva NT, Morris JH, Bork P, Jensen LJ, Mering CV. STRING v11: protein-protein association networks with increased coverage, supporting functional discovery in genome-wide experimental datasets. Nucleic Acids Res. 2019 Jan 8;47(D1):D607-D613. doi: 10.1093/nar/gky1131.
12. Shannon P, Markiel A, Ozier O, Baliga NS, Wang JT, Ramage D, Amin N, Schwikowski B, Ideker T. Cytoscape: A software environment for integrated models of biomolecular interaction networks. Genome Res. 2003 Nov;13(11):2498-504. doi: 10.1101/gr.1239303.
13. Chin CH, Chen SH, Wu HH, Ho CW, Ko MT, Lin CY. CytoHubba: Identifying hub objects and sub-networks from complex interactome. BMC Syst Biol. 2014;8(Suppl 4):S11.
14. Morris GM, Lim-Wilby M. Molecular docking. Methods Mol Biol. 2008;443:365–382.) (Ferreira LG, dos Santos RN, Oliva G, Andricopulo AD. Molecular docking and structure-based drug design strategies. Molecules. 2015;20(7):13384–13421.
15. O. Trott, A. J. Olson. AutoDock Vina: improving the speed and accuracy of with a new scoring function, efficient optimization and multithreading. Journal of Computational Chemistry 31 (2010) p. 455-461 DOI 10.1002/jcc.21334) (Forli S, Huey R, Pique ME, Sanner MF, Goodsell DS, Olson AJ. Computational protein–ligand docking and virtual drug screening with the AutoDock suite. Nat Protoc. 2016;11(5):905–919.
16. Widden, H., Placzek, W.J. The multiple mechanisms of MCL1 in the regulation of cell fate. Commun Biol 4, 1029 (2021). https://doi.org/10.1038/s42003-021-02564-6.
17. Macleod, T., Doble, R., McGonagle, D., Wasson, C., Alase, A., Stacey, M., & Wittmann, M. Neutrophil Elastase-mediated proteolysis activates the anti-inflammatory cytokine IL-36 Receptor antagonist. Scientific Reports. 2016; 6. https://doi.org/10.1038/srep24880.
18. Zeng, W., Song, Y., Wang, R., He, R., & Wang, T. Neutrophil elastase: From mechanisms to therapeutic potential. Journal of Pharmaceutical Analysis. 2023; 13. https://doi.org/10.1016/j.jpha.2022.12.003.
19. Başar Kılıç Ş, Taheri S, Mehmetbeyoğlu Duman E, Öksüm Solak E, Yılmaz Şükranlı Z, Rassoulzadegan M, Borlu M. Psoriatic skin transcript phenotype: androgen/estrogen and cortisone/cortisol imbalance with increasing DNA damage response. Mol Biol Rep. 2024 Aug 24;51(1):933. doi: 10.1007/s11033-024-09782-1. PMID: 39180588.
20. Fu, Z., He, Y., Gao, L., Tong, X., Zhou, L., & Zeng, J. STAT2/Caspase3 in the diagnosis and treatment of psoriasis. European Journal of Clinical Investigation. 2023; 53. https://doi.org/10.1111/eci.13959.

21. Sur, S., & Agrawal, D. Phosphatases and kinases regulating CDC25 activity in the cell cycle: clinical implications of CDC25 overexpression and potential treatment strategies. Molecular and Cellular Biochemistry. 2016; 416. https://doi.org/10.1007/s11010-016-2693-2.
22. Liu, K., Zheng, M., Lu, R., Du, J., Zhao, Q., Li, Z., Li, Y., & Zhang, S. The role of CDC25C in cell cycle regulation and clinical cancer therapy: a systematic review. Cancer Cell International. 2020; 20. https://doi.org/10.1186/s12935-020-01304-w.
23. Gelmi, M., Houtzagers, L., Strub, T., Krossa, I., & Jager, M. MITF in Normal Melanocytes, Cutaneous and Uveal Melanoma: A Delicate Balance. International Journal of Molecular Sciences. 2022; 23. https://doi.org/10.3390/ijms23116001.